

QCD radiative correction to pair-annihilation of spin-1 bosonic Dark Matter

Jae Ho Heo*

*Physics Department University of Illinois at Chicago and
845 West Taylor Street, Chicago, Illinois, 60607*

The next-to-leading order (NLO) QCD corrections are calculated to pair-annihilation of spin-1 bosonic dark matter (DM) by dimensionally regularizing both ultraviolet and infrared singularities in non-relativistic ($v \ll 1$) limit. The complete $O(\alpha_s)$ correction is about 8% in the case considered only massless gluon and about 13%, when included the massive gluon at 1TeV. The NLO QCD correction could shift the DM mass window constrained by WMAP and improve the observability in the projected direct detector, GENIUS.

I. INTRODUCTION

The hypercharge gauge boson (B') could play the role of dark matter with the right properties in some certain types of models with Z_2 -symmetry. Amongst them, the most appealed models are universal extra dimensions (UED) [1] and Little Higgs (LH) [2] with the rigorous theoretical frame work (hierarchy problem). The phenomenology of the dark matter candidate were studied well in classical limit. However, the empirical advances in cosmology and astrophysics and the advent of new era in particle physics at LHC inspire studying beyond the leading order. We present the next-to-leading order (NLO) QCD corrections to pair-annihilation of spin-1 bosonic dark matter by dimensionally regularizing both ultraviolet (UV) and infrared (IR) singularities in the non-relativistic ($v \ll 1$) limit. No particular model is assumed, but the parity (Z_2 -symmetry) and the parity partners are considered.

Fig.1 shows the Born diagrams. The internal bold line is the parity (Z_2 -symmetry) partner of the outgoing quarks. The amplitude for Born diagrams is given by

$$\mathcal{M}_B = -g_Y^2 Y_L^2 \bar{u}(p_2) \left(\gamma^\mu \frac{\not{p}_2 - \not{p}_1 + \widetilde{M}}{t - \widetilde{M}^2} \gamma^\nu + \gamma^\nu \frac{\not{p}_2 - \not{p}'_1 + \widetilde{M}}{u - \widetilde{M}^2} \gamma^\mu \right) P_L v(p'_2) \epsilon_\mu(p_1) \epsilon_\nu(p'_1) + \text{RH} \quad (1)$$

—where g_Y is the hypercharge coupling, Y_L is hypercharge for left-chiral quark, \widetilde{M} is mass of the intermediated heavy

*Electronic address: jheo1@uic.edu

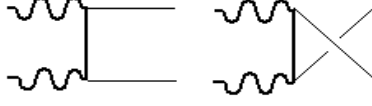


FIG. 1: The Born diagrams for $B'B' \rightarrow q\bar{q}$.

quark, t and u are the relevant Mandelstam parameters, P_L is a left-handed projector and RH stands for the right handed part ($L \leftrightarrow R$).

In the extremely non-relativistic limit ($v \simeq 0$), $p_1 \simeq p'_1 \simeq (p_2 + p'_2)/2 \simeq (M, \mathbf{0})$. The invariant Mandelstam parameters are

$$s = (p_1 + p'_1)^2 = (p_2 + p'_2)^2 \simeq 4M^2 \quad (2a)$$

$$t = (-p_1 + p_2)^2 = (p'_1 - p'_2)^2 \simeq -M^2 \quad (2b)$$

$$u = (-p'_1 + p_2)^2 = (p_1 - p'_2)^2 \simeq -M^2 \quad (2c)$$

where M is the mass of hypercharge gauge boson (B').

The formulae reduces to

$$\mathcal{M}_B = g_Y^2 Y_L^2 \bar{u}(p_2) \frac{(p_2 - p'_2)^\mu \gamma^\nu + (p_2 - p'_2)^\nu \gamma^\mu}{M^2 + \widetilde{M}^2} P_L v(p'_2) \epsilon_\mu(p_1) \epsilon_\nu(p'_1) + \text{RH} \quad (3)$$

The consistent annihilation rate in $d = 4 - 2\epsilon$ is

$$\sigma_B v = \frac{(1 - \epsilon)\Gamma(1 - \epsilon)}{\Gamma(2 - 2\epsilon)} \left(\frac{4\pi\mu^2}{4M^2} \right)^\epsilon \frac{2g_Y^4 (Y_L^4 + Y_R^4) N_c}{9\pi} \frac{M^2}{(M^2 + \widetilde{M}^2)^2} \quad (4)$$

where N_c is degrees of color, v denotes the relative velocity between hypercharge gauge boson pair, μ is an arbitrary mass scale and σ_B is the Born cross section.

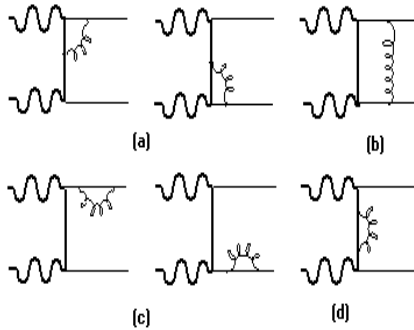


FIG. 2: The Feynman diagrams which contribute to the next-to-leading order (NLO) QCD virtual radiative correction($B'B' \rightarrow q\bar{q}$). The crossed (u -channel) diagrams are not displayed.

II. NEXT-TO-LEADING ORDER CALCULATION

The one-loop amplitudes consist of the virtual corrections Fig.2(a),(b) and the counterterm contributions Fig.2(c),(d), which the vertex and propagator corrections are related by the Ward-Takahashi identity. Adding up both contributions must be ultraviolet finite. The amplitudes contain infrared divergences due to massless gluon virtual exchange. The infrared should cancel exactly against the one present in the gluon final state radiation, Fig.3(a),(b),(c). The method is to use dimensional regularization in $d = 4 - 2\epsilon$ with massless on-shell quarks to regularize both types of divergences, UV and IR divergences. The individual diagrams are calculated in the renormalizable Feynman gauge (the gauge parameter, $\xi = 1$), which provides the gluon propagator. All of new particles are set up to have the same mass for convenience and the decoupling occurred by the large mass difference between new particles is not considered.

A. Virtual corrections

In extremely non-relativistic ($v \simeq 0$) and massless outgoing particle limits, all of the virtual corrections could be expressed by two form factors¹ related to tensors, $(p_2 - p'_2)^\mu \gamma^\nu + (p_2 - p'_2)^\nu \gamma^\mu$ and $(p_2 + p'_2)^\mu \gamma^\nu + (p_2 + p'_2)^\nu \gamma^\mu$. However $(p_2 - p'_2)^\mu \gamma^\nu + (p_2 - p'_2)^\nu \gamma^\mu$ only survives. $p_2 + p'_2$ is a time-like vector, so it disappears as contracting B' polarizabilities, $\epsilon_\mu(p_1)$ and $\epsilon_\nu(p'_1)$, which are the space-like vectors. Thus the virtual corrections could be expressed

¹ Two more form factors are possible, which are related to the tensors $(\not{p}_2 \pm \not{p}'_2)g^{\mu\nu}$. But both don't give any contribution in the massless outgoing particle limit.

with only one form factor, which is the coefficient of Born amplitude.

$$\mathcal{M}_1 = F_{B'} \mathcal{M}_B \quad (5)$$

We use the conventional approach by Feynman parameters to calculate the corrections. The virtual corrections are simplified in the common integral with the shifted momentum and Feynman parameters, and the infrared divergences appear in the Feynman parameter integrations.

$$\int \frac{d^d \ell dx_i}{(2\pi)^d} \delta(\sum x_i - 1) \frac{(\ell^2)^r}{(\ell^2 - C)^m} = \frac{i(-1)^{r-m}}{(4\pi)^{d/2}} \frac{\Gamma(r + d/2) \Gamma(m - r - d/2)}{\Gamma(d/2) \Gamma(m)} \int dx_i \delta(\sum x_i - 1) C^{r-m+d/2} \quad (6)$$

The amplitude of the diagrams in Fig.1(a) is

$$\mathcal{M}_{1,L} = -g_Y^2 Y_L^2 \bar{u}(p_2) \left[\Gamma^\mu \left(\frac{\not{p}_2 - \not{p}_1 + M}{t - M^2} \right) \gamma^\nu + \gamma^\mu \left(\frac{\not{p}_2 - \not{p}_1 + M}{t - M^2} \right) \Gamma^\nu + \mu \leftrightarrow \nu \right] P_L v(p'_2) \epsilon_\mu(p_1) \epsilon_\nu(p'_1) \quad (7)$$

Γ^μ and Γ^ν are the vertex corrections in d -dimensions, which are given by

$$\Gamma^\mu = -ig_s^2 C_F \int \frac{d^d k}{(2\pi)^d} \frac{\gamma^\rho (\not{p}_2 + \not{k}) \gamma^\mu (\not{p}_2 - \not{p}_1 + \not{k} + M) \gamma_\rho}{k^2 (p_2 + k)^2 ((p_2 - p_1 + k)^2 - M^2)} \quad (8a)$$

$$\Gamma^\nu = -ig_s^2 C_F \int \frac{d^d k}{(2\pi)^d} \frac{\gamma^\rho (\not{p}'_1 - \not{p}_2 + \not{k} + M) \gamma^\nu (-\not{p}'_2 + \not{k}) \gamma_\rho}{k^2 (-p'_2 + k)^2 ((p'_1 - p'_2 + k)^2 - M^2)} \quad (8b)$$

where g_s is the strong coupling and C_F is Casimir operator of the fundamental representation in the color gauge group.

The form factor of Fig.1(a) results in

$$F_{B'} = \frac{\alpha_s C_F}{2\pi} \left(\frac{4\pi\mu^2}{4M^2} \right)^\epsilon \Gamma(1 + \epsilon) \left(\frac{1}{\epsilon_{UV}} + 1 + \log 2 \right) \quad (9)$$

where the subscript UV implies the $1/\epsilon$ pole by UV divergence and α_s is QCD fine structure constant.

Calculations² of Fig.1 (b) are tedious and require being very careful since the number of propagators in the loop are four and it involves a three folded integral over Feynman parameters. The scattering amplitude is given by

$$\mathcal{M}_{1,L} = -g_Y^2 Y_L^2 \bar{u}(p_2) \Gamma^{\mu\nu} P_L v(p'_2) \epsilon_\mu(p_1) \epsilon_\nu(p'_1) \quad (10)$$

where $\Gamma^{\mu\nu}$ is the vertex correction for t and u -channels and is written as

$$\Gamma^{\mu\nu} = -ig_s^2 C_F \int \frac{d^d k}{(2\pi)^d} \frac{\gamma^\rho (\not{p}_2 + \not{k}) \gamma^\mu (\not{p}_2 - \not{p}_1 + \not{k} + M) \gamma^\nu (-\not{p}'_2 + \not{k}) \gamma_\rho + \mu \longleftrightarrow \nu}{k^2 (p_2 + k)^2 (-p'_2 + k)^2 ((p_2 - p_1 + k)^2 - M^2)} \quad (11)$$

This integration could also be manipulated into the common form, Eq.(6), however the integral has singularity in the euclidean region. The imaginary parts are included to continue this integral in the euclidean region for the positive s .

$$F_{B'} = \frac{\alpha_s C_F}{2\pi} \left(\frac{4\pi\mu^2}{4M^2} \right)^\epsilon \Gamma(1+\epsilon) \left(-\frac{1}{\epsilon_{IR}^2} - \frac{2}{\epsilon_{IR}} - \frac{14}{3} + \frac{2}{3} \log 2 + \frac{2\pi^2}{3} + i\pi \left(\frac{1}{\epsilon_{IR}} + 3 + \frac{\pi}{6} \right) \right) \quad (12)$$

The imaginary parts could be neglected by S-matrix unitary condition for real radiative measurements.

The contribution of Fig.1(c) comes from propagator corrections to on-shell quark lines. For the massless quark lines, there is no contribution using dimensional regularization since the same regulator is used. Considering the leading order of ϵ , it can be written as

$$F_{B'} = \frac{\alpha_s C_F}{2\pi} \left(\frac{4\pi\mu^2}{4M^2} \right)^\epsilon \Gamma(1+\epsilon) \left(-\frac{1}{2\epsilon_{UV}} + \frac{1}{2\epsilon_{IR}} \right) \quad (13)$$

However the contribution of Fig.1(d) comes from off-shell heavy quark lines. It produces an amount of contribution without IR divergence.

² The analogous calculation for the box diagram are in Ref.[3] for the different phenomenology.

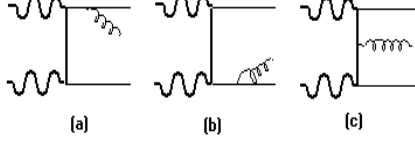


FIG. 3: The Feynman diagrams which contribute to the next-to-leading order (NLO) QCD real radiative correction($B'B' \rightarrow gq\bar{q}$). The crossed (u -channel) diagrams are not displayed

$$F_{B'} = 2 \frac{d\Sigma_2}{d\not{p}} \Big|_{p^2=-M^2} = \frac{\alpha_s C_F}{2\pi} \left(\frac{4\pi\mu^2}{4M^2} \right)^\epsilon \Gamma(1+\epsilon) \left(-\frac{1}{2\epsilon_{UV}} - 1 + \log 2 \right) \quad (14)$$

where the factor 2 comes from two vertices and those give the identical contribution. The results show that UV divergences are exactly canceled by the counter diagrams.

Adding up all of the virtual corrections, the QCD corrections are

$$\delta_{QCD} = 2 \text{Re}(F_{B'}) = \frac{\alpha_s C_F}{\pi} \left(\frac{4\pi\mu^2}{4M^2} \right)^\epsilon \Gamma(1+\epsilon) \left(-\frac{1}{\epsilon_{IR}^2} - \frac{3}{2\epsilon_{IR}} + \frac{2\pi^2}{3} - \frac{14}{3} + \frac{8}{3} \log 2 \right) \quad (15)$$

B. Real corrections

The real QCD correction appears in the ratio of annihilation rates for two and three body final states. Integrating over the polarization of the incoming vector bosons and summing over the spin and color of outgoing quark and gluon, the annihilation rate for three body final states is

$$\sigma v = \frac{1}{4M^2} \cdot \frac{N_C}{9} \int d\Phi_3 |\mathcal{M}_a + \mathcal{M}_b + \mathcal{M}_c|^2 \quad (16)$$

$\mathcal{M}_a, \mathcal{M}_b$ and \mathcal{M}_c are the scattering amplitudes corresponded to the diagrams (a),(b),(c) of Fig.3, and are given by

$$\mathcal{M}_{a,L} = -ig_Y^2 g_s Y_L^2 T^a \frac{\bar{u}(p_2) \gamma^\rho (\not{p}_2 + \not{k}) (\gamma^\mu \not{p}_a \gamma^\nu + \gamma^\nu \not{p}_a \gamma^\mu) P_L v(p'_2) \epsilon_\mu(p_1) \epsilon_\nu(p'_1) \epsilon_\rho^{*a}(k)}{(p_2 + k)^2 (p_a^2 - M^2)} \quad (17a)$$

$$\mathcal{M}_{b,L} = -ig_Y^2 g_s Y_L^2 T^a \frac{\bar{u}(p_2) (\gamma^\mu \not{p}_b \gamma^\nu + \gamma^\nu \not{p}_b \gamma^\mu) (-\not{p}'_2 - \not{k}) \gamma^\rho P_L v(p'_2) \epsilon_\mu(p_1) \epsilon_\nu(p'_1) \epsilon_\rho^{*a}(k)}{(-p'_2 - k)^2 (p_b^2 - M^2)} \quad (17b)$$

$$\mathcal{M}_{c,L} = -ig_Y^2 g_s Y_L^2 T^a \frac{\bar{u}(p_2) [\gamma^\mu \not{p}_b \gamma^\rho \not{p}_a \gamma^\nu + M^2 \gamma^\mu \gamma^\rho \gamma^\nu + \mu \leftrightarrow \nu] P_L v(p'_2) \epsilon_\mu(p_1) \epsilon_\nu(p'_1) \epsilon_\rho^{*a}(k)}{(p_a^2 - M^2)(p_b^2 - M^2)} \quad (17c)$$

where T^a is the QCD generator and $p_a = p'_1 - p'_2 = -p_1 + p_2 + k, p_b = -p_1 + p_2 = p'_1 - p'_2 - k$ in shorthand and $p_1 \simeq p'_1 \simeq (p_2 + p'_2 + k)/2$ in the non-relativistic limit. The numerator of \mathcal{M}_c is allowed to express by the momentum, $p = p_2 - p'_2$ and k on the diagrammatic symmetry.

$$\mathcal{N}_c = p^\rho (p^\mu \gamma^\nu + p^\nu \gamma^\mu) + ip_\sigma k_\delta \gamma^5 \epsilon^{\sigma\rho\delta\lambda} (g_\lambda^\mu \gamma^\nu + g_\lambda^\nu \gamma^\mu - g^{\mu\nu} \gamma_\lambda) + (p_2 \cdot p'_2 + 2M^2) (g^{\mu\rho} \gamma^\nu + g^{\nu\rho} \gamma^\mu - g^{\mu\nu} \gamma^\rho) \quad (18)$$

So $\epsilon_\mu \epsilon_\nu^* = -g_{\mu\nu}$ is adopted to calculate the squared amplitude for both incoming massive hypercharge gauge bosons in Feynman gauge since the polarization vectors $\epsilon_\mu(p_1), \epsilon_\nu(p'_1)$ are space-like. The soft and collinear singularities appear at the squared amplitudes, $|\mathcal{M}_a|^2, |\mathcal{M}_b|^2, 2\text{Re}(\mathcal{M}_a^* \mathcal{M}_b)$. $1/\epsilon$ poles are canceled out at $2\text{Re}(\mathcal{M}_a^* \mathcal{M}_c)$ and $2\text{Re}(\mathcal{M}_b^* \mathcal{M}_c)$ as combining the numerator and denominator, and $|\mathcal{M}_c|^2$ is totally free of IR divergences.

The new dimensionless parameters are introduced for the phase space integration by the energy-momentum conservation for convenience.

$$x_1 = \frac{p_2 \cdot k}{2M^2}, \quad x_2 = \frac{p'_2 \cdot k}{2M^2}, \quad x_3 = \frac{p_2 \cdot p'_2}{2M^2} \quad (19)$$

$1/\epsilon$ poles appear at $x_1 = 0$ and $x_2 = 0$. The Lorentz invariant three body phase space integral with the new parameters is given by

$$\int d\Phi_3 = \frac{4M^2}{(4\pi)^3 \Gamma(2 - 2\epsilon)} \left(\frac{4\pi\mu^2}{4M^2} \right)^{2\epsilon} \int dx_1 dx_2 dx_3 (x_1 x_2 x_3)^{-\epsilon} \delta(\sum x_i - 1) \quad (20)$$

The real correction gives

$$\delta_{QCD} = \frac{\alpha_s C_F}{\pi} \left(\frac{4\pi\mu^2}{4M} \right)^\epsilon \Gamma(1+\epsilon) \left(\frac{1}{\epsilon_{IR}^2} + \frac{3}{2\epsilon_{IR}} + \frac{39}{4} - \frac{7}{6}\pi^2 \right) \quad (21)$$

Adding up all of the contributions³, the infrared are exactly canceled and the finite result is

$$\delta_{QCD} = \frac{\alpha_s C_F}{\pi} \left(\frac{61}{12} + \frac{8}{3} \log 2 - \frac{\pi^2}{2} \right) \quad (22)$$

The correction is about 8% enhancement for $C_F = 4/3$ and $\alpha_s(1\text{TeV}) = 0.09$ and the finiteness of this correction implies that there is no divergence by degeneracy.

C. The corrections by heavy gluon

For the heavy gluon which has odd parity, the internal quark lines have to be switched in Fig.1. There is an amount of constant correction for the massless quark line since there are no IR divergences. UV divergences are exactly canceled out with the counter diagrams. A massive gluon could not be produced by parity (Z_2 -symmetry), so there are no real corrections and it results in the improved QCD correction. The QCD corrections by heavy gluon could also be calculated fully analytically and the overall correction is given by

$$\delta_{QCD} = \frac{\alpha_s C_F}{\pi} \left(-5 + \frac{9\pi^2}{8} - 10 \log 2 + \frac{7\pi}{6\sqrt{3}} \right) \quad (23)$$

The correction is about 5% enhancement and it is comparable to massless gluon correction.

III. APPLICATIONS TO PHENOMENOLOGY

The hypercharge gauge boson (B') has been a good dark matter candidate in UED and LH, but both models were extended in different ways. The dimensions are enlarged for UED with the same gauge structure as SM, otherwise the

³ The corrections also can be approached by optical theorem to acquire the cross section. But eventually both are identical and we would have the same QCD correction.

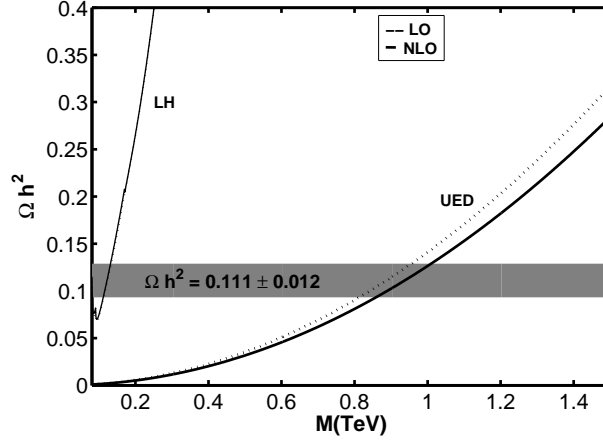


FIG. 4: Prediction for relic abundance as a function of the WIMP mass. NLO QCD radiative correction is considered on the bold lines. The horizontal band denotes $\Omega h^2 = 0.111 \pm 0.012$ and defines the WIMP mass window.

symmetry groups are enlarged for LH in 4-dimension. So the mass of new particles are scaled by the extra dimension size R compactified on an S^1/Z_2 orbifold for UED and the enlarged global symmetry breaking scale f for LH. Since the new particles are in the different symmetry group structure, the UED and LH gauge boson have the different hypercharges of the fermion and it causes them to induce the different phenomenological signatures.

The DM relic abundance is determined by the behavior of the pair-annihilation rates in the non-relativistic limit. The UED candidate mainly annihilates into fermion pairs, charged leptons, quarks and neutrinos. Otherwise, annihilation into fermions for LH is highly suppressed by small value ($\tilde{Y} = 1/10$) of hypercharge. The detailed quantitative analyses for relic abundance by this type of WIMP annihilations are in Ref.[4] for UED and Ref.[5] for LH. Fig.4 shows the prediction for relic abundance as a function of WIMP mass with the present WMAP precision [6] for UED and LH. The mass window are shifted about 50 GeV compared to the leading order for UED⁴.

The elastic scattering for the direct detection has the same amount of QCD radiative correction as the pair annihilation. Fig.2, 3 show WIMP annihilation into quarks. But if reading from bottom to top, it describes the elastic scattering, which we can consider at direct DM detectors. The elastic scattering is well analyzed in Ref.[7] for UED and in Ref.[5] for LH. Fig.5 shows predicted spin-dependent and independent nucleon cross section, where $\Delta = (\tilde{M} - M)/M$ denotes the fractional mass difference for UED, and Fig.6 for LH with present (CDMS-II [8]) and projected (GENIUS (for SI) [9], NAIAD (for SD) [10]) experimental sensitivities. Spin-independent (SI) cross sections are suppressed relative to spin-dependent (SD) ones by $\sim m_p/M$. The predictions are well below experimental sensitivities, and our

⁴ It was truncated to the first level Kaluza Klein (KK) mode for our calculation and UED with such truncation is renormalizable though the theory is not renormalizable.

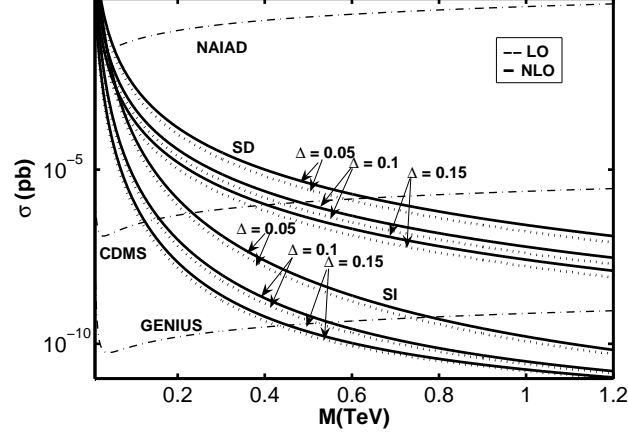


FIG. 5: Predicted spin-dependent and independent nucleon cross sections with the present (CDMS) and projected (GENIUS, NAIAD) experimental sensitivities in UED. NLO QCD corrections are considered on the bold lines. $m_h=120\text{GeV}$ is assumed. The lines are labeled by the values of $\Delta = 0.05, 0.1, 0.15$ from top to bottom.

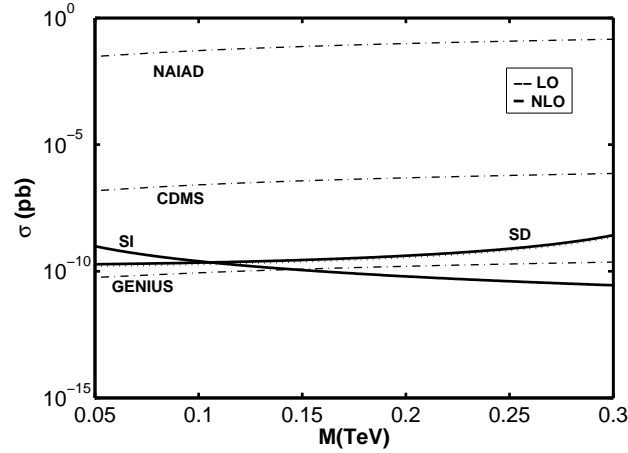


FIG. 6: Predicted spin-dependent and independent nucleon cross sections with the present (CDMS) and projected (GENIUS, NAIAD) experimental sensitivities in LH. NLO QCD corrections are considered on the bold lines. $m_h=120\text{GeV}$ and $\widetilde{M} = 350\text{GeV}$ are assumed.

QCD correction improves the WIMP observability in the projected dectector SuperCDMS (GENIUS).

IV. CONCLUSION

The next-to-leading order (NLO) QCD corrections are calculated to pair-annihilation of spin-1 bosonic dark matter by dimensionally regularizing both ultraviolet and infrared singularities in non-relativistic limit. The order α_s correction amounts to about 8% and can enhance to 13%, when considered heavy gluon. The possible DM mass window

could be shifted and the observability could be improved.

APPENDIX: USEFUL FORMULA AND IDENTITIES

The Dirac algebra in $d = 4 - 2\epsilon$ dimensions are well listed in Ref.[11]. They could be followed by the anticommutator $\{\gamma^\mu, \gamma^\mu\} = g^{\mu\nu}$ and the identity $\gamma^\mu \gamma_\mu = d$. The regulator ϵ is omitted on trace algebra $\text{Tr}[\mathbf{I}] = 2^{d/2}$ for two and three body cross section calculation.

$1/\epsilon_{IR}$ poles are extracted by the partial integrations on the loop calculations in case of need to do the poles and the remnants are expanded in ordinary Taylor series with respect to ϵ . The three folded parametric integrals for the box diagram are calculated by Feynman parameter properties, since one of them is not symmetric with the others.

$$\int_0^1 dx \int_0^{1-x} dy f(x, y) = \int_0^1 dy \int_0^{1-y} dx f(x, y) \quad (\text{A.1})$$

The complicated integrations are avoided and number of integrations are reduced with this property.

The useful identity to split the singular and non-singular parts for the real corrections is

$$\frac{1}{x(1-x)} = \frac{1}{x} + \frac{1}{1-x} \quad (\text{A.2})$$

This identity can be extended to the higher powers of the variables and will simplify the calculations since the regulator ϵ can be dropped for non-singular parts.

Some of the parametric integrals contain the dilogarithm (or spence) function.

$$\text{Li}_2(x) \equiv - \int_0^1 dt \frac{\log(1 - xt)}{t} \quad (\text{A.3})$$

The values which appear in our calculations

$$\text{Li}_2(1) = \frac{\pi^2}{6} \quad (\text{A.4a})$$

$$\text{Li}_2(-1) = -\frac{\pi^2}{12} \quad (\text{A.4b})$$

$$\text{Li}_2\left(\frac{1}{2}\right) = \frac{\pi^2}{12} - \frac{\log^2 2}{2} \quad (\text{A.4c})$$

The parametric integrals which appeared in the box diagrams reduce to the incomplete beta function.

$$B_{1/2}(m, n) \equiv \int_0^{1/2} dx x^{m-1} (1-x)^{n-1} \quad (\text{A.5})$$

$$B_{1/2}(m, n) + B_{1/2}(n, m) = B(m, n) \quad (\text{A.6a})$$

$$B_{1/2}(m, m) = \frac{1}{2} B(m, m) \quad (\text{A.6b})$$

$$B_{1/2}(m, m+1) = \frac{1}{2} \left[B(m, m+1) + \frac{2^{-2m}}{m} \right] \quad (\text{A.6c})$$

$$B_{1/2}(m, m+2) = \frac{1}{2} \left[B(m, m+2) + \frac{2^{-2m}}{m} \right] \quad (\text{A.6d})$$

where

$$B(m, n) = \frac{\Gamma(m)\Gamma(n)}{\Gamma(m+n)} \quad (\text{A.7})$$

For integer n , the Taylor expansion is adopted with respect to ϵ .

$$B_z(-\epsilon, 0) = 1 + \epsilon \log(1 - z) - \epsilon^2 \text{Li}_2(z) \quad (\text{A.8a})$$

$$B_z(-\epsilon, 1) = 1 + \epsilon \left(-\frac{z}{1-z} + \log(1-z) \right) + \epsilon^2 (\log(1-z) - \text{Li}_2(z)) \quad (\text{A.8b})$$

with $z = 1/2$.

The parametric integrations involved the heavy gluon loops are

$$\begin{aligned} \int_0^1 dx \log(x^2 - x + 1) &= 2 \left(\frac{\sqrt{3}}{6} \pi - 1 \right) \\ \int_0^1 dx (x^2 - x) \log(x^2 - x + 1) &= \frac{17}{18} - \frac{\sqrt{3}}{6} \pi \\ \int_0^1 dx \frac{x^2 - x}{x^2 - x + 1} &= -1 + \frac{2}{3\sqrt{3}} \pi \end{aligned}$$

-
- [1] T. Appelquist, H. C. Cheng and B. A. Dobrescu, Phys. Rev. D **64**, 035002 (2001)[arXiv:hep-ph/0012100]
 - [2] N. Arkani-Hamed, A. G. Cohen, E. Katz, and A. E. Nelson, JHEP **07**, 034 (2002); H. C. Cheng and I. Low, JHEP **0309**, 051 (2003)[arXiv:hep-ph/0308199] ; JHEP **0408**, 061 (2004)[arXiv:hep-ph/0405243]; I. Low, JHEP **0410**, 067 (2004)[arXiv:hep-ph/0409025]
 - [3] K. Hagiwara, C.B. Kim and T. Yoshino, Nuclear Physics B **177**, 461 (1981); B. Mele, P. Nason and G. Ridolfi. Nuclear Physics B **357**, 409 (1991)
 - [4] G. Servant, T. M. P. Tait, Nucl. Phys. B **650**, 391 (2003) [arXiv:hep-ph/0206071]; K. Kong and K.T. Matchev, JHEP **0601**, 038 [arXiv:hep-ph/0509119]
 - [5] Andreas Birkedal, Andrew Noble, Maxim Perelstein, and Andrew Spray, Phys. Rev D **74**, 035002 (2006)[arXiv:hep-ph/0603077]
 - [6] D. N. Spergel *et al.*, [WMAP Collaboration], Astrophys. J Suppl. **170**, 377 (2007) [arXiv:astro-ph/0603449]
 - [7] H. C. Cheng, J. L. Feng and K. T. Matchev, Phys. Rev. Lett **89**, 211301 (2002)[arXiv:hep-ph/0207125]; G. Servant and T. M. P. Tait, New J. of Phys **4**, 99.1 (2002)[arXiv:hep-ph/0209262]; T. G. Rizzo, Phys. Rev. D **64**, 095010 (2001)[arXiv:hep-ph/0106336]

- [8] D. S. Akerib *et al.*, [CDMS Collaboration], Phys. Rev. Lett. **96**, 011302 (2006)[arXiv:astro-ph/050929]
- [9] P. L. Brink, B. Cabrera, C.L. Chang, J. Cooley and R. W. Ogburn [arXiv:astro-ph/0503583]
- [10] N. J. C. Spooner *et al.*, Phys. Lett. B **473**, 330 (2000)
- [11] W. J. Marciano, Phys. Rev. D **12**, 3861 (1975), "Dimensional regularization is well explained in this letter"